Simulation of Plasma Interaction with Io's Atmosphere

Chris H. Moore[a], Hao Deng[b], David B. Goldstein[a], Deborah Levin[b], Philip L. Varghese[a], Laurence M. Trafton[a], Bénédicte D. Stewart[a], and Andrew C. Walker[a]

[a]*University of Texas at Austin, Center for Aeromechanics Research, 1 University Station C0600 Austin, TX 78712*
[b]*Pennsylvania State University, Department of Aerospace Engineering, 229 Hammond, University Park, PA 16802*

Abstract. One dimensional Direct Simulation Monte Carlo (DSMC) simulations are used to examine the interaction of the jovian plasma torus with Io's sublimation atmosphere. The hot plasma sweeps past Io at ~57 km/s due to the external Jovian magnetic and corotational electric fields and the resultant energetic collisions both heat and dissociate the neutral gas creating an inflated, mixed atmosphere of SO_2 and its daughter products. The vertical structure and composition of the atmosphere is important for understanding Io's mass loading of the plasma torus, electron excited aurora, and Io's global gas dynamics. Our 1D simulations above a fixed location on the surface of Io allows the O^+ and S^+ ions to drift down into the domain where they then undergo elastic and charge exchange collisions with the neutral gas. Each electron's position is determined by the motion of a corresponding ion; however, the electrons retain their own velocity components which are then used during elastic, ionization, and dissociation collisions with the neutral gas. Charge exchange creates fast neutral O and S atoms. Molecular Dynamic/Quasi–Classical Trajectory (MD/QCT) calculations are used to generate total and reaction cross sections for energetic $O+SO_2$ collisions [1] as well as for $O+O_2$ collisions. In addition, the model accounts for photo-dissociation assuming the atmosphere is optically thin. Our previous plasma heating model (without chemistry) agrees well with the vertical structure of the current model at lower altitudes where the gas is collisional; however, at high altitudes (>100 km) significant differences among the models appear. The current model's constant **E** and **B** fields results in reacceleration of the ions and electrons to a constant **E**×**B** drift velocity towards the surface after collisions with the neutral gas and, while the results are an upper limit on the plasma interaction strength, the results indicate that joule heating is significant, causing large changes in the vertical structure of the atmosphere. Plasma heating of, not momentum transfer to, the atmosphere dominates even for radially inward plasma flows resulting in a hot, inflated atmosphere. The scale heights for the various species were found to be a competition between the hydrodynamic scale height based on the gas constant (for the mixture if collisional) and the production rate from dissociation of SO_2 which depends on the local SO_2 density and available plasma energy at that altitude.

Keywords: Io, Atmospheric dynamics, Plasma
PACS: 96.12.Jt, 96.12.Wx, 96.30.lb

INTRODUCTION

Io's surface is partially covered with SO_2 frost that sustains a collisional sublimation atmosphere near the surface. In addition to atmospheric variability from volcanic activity, the local sublimation SO_2 gas density varies strongly depending on the local surface temperature and the presence of frost, among other parameters [2]. Io's dayside atmosphere ranges from continuum near the surface with a mean free path of ~10 m and an atmospheric scale height of ~8 km, to fully rarefied above ~100 km where the mean free path is >1 km. Significant atmospheric escape can occur above the exobase (which ranges from 200–400 km) due to collisional sputtering by the energetic jovian plasma which sweeps past Io at ~57 km/s. This plasma also partially dissociates the neutral gas, creating the dissociation products SO, O_2, O, and S. In the collisional part of the atmosphere the neutral species maintain a single scale height based on the mixture gas constant; however, once the flow is sufficiently collisionless at higher altitudes it is expected that the species will separate out and their scale heights will be determined by each species' mass.

Previous 1-D simulations examined the effect of plasma heating on the vertical structure and atmospheric loss rate [3] and the effect of non-condensables on the atmospheric dynamics during eclipse [4]. 2-D computational work on Io's atmosphere has modeled Io's steady-state atmosphere including crude plasma heating [5] and plasma chemistry models that have found a dayside SO/SO_2 ratio of 3-7% [6], consistent with an observed ratio of 1-10% [7]. More recent 3-D DSMC simulations of Io's atmosphere [8] improved on previous simulations by using a complex surface temperature and frost fraction model but still used a simple plasma heating model without

chemistry. The present work aims to investigate the vertical structure and composition of Io's atmosphere by incorporating an improved plasma model that includes resonant charge exchange [9], electron elastic, ionization, and dissociation collisions [10], and MD/QCT dissociation cross sections [1, 11] for fast neutrals.

A more accurate atmospheric model is critical in order to understand Io's electrodynamic interaction with the Jupiter plasma torus and the resulting auroral emissions from electron excitation of the neutral species, SO_2, S_2, SO, O_2, O, and S. The vertical structure and composition of Io's atmosphere will influence sputtering and the supply rate of material to the plasma torus [12] which itself then effects the electrodynamic interaction through ion mass loading. In addition, the intensity and morphology of Io's auroral glows generated by photon and electron impact excitation of the atmosphere are affected by the atmosphere's vertical structure [10]. Non-condensables (O_2 and possibly SO), formed via plasma and photo-dissociation of the sublimated SO_2, have been found to dramatically influence the rate of atmospheric freeze-out during eclipse via the formation of a non-condensable diffusion layer [4]. Furthermore, non-condensables are also swept to the cold, low pressure night side by the circumplanetary winds where they then build up and create sufficient back pressure to reduce the steady state wind speed [5]. Previous work [4,5] investigating the effect of non-condensables have neglected plasma chemistry and its role as a loss mechanism for the non-condensable gas.

MODEL

Our computation simulates the dayside atmospheric dynamics above an SO_2 frost-covered location (at a fixed longitude and latitude) on Io's surface as the warm surface sublimates SO_2 which is then heated and dissociated by the torus plasma and sunlight. The resultant atmosphere was simulated by a one-dimensional multi-species model using the DSMC method [13]. The general details of the code and its application are discussed in previous papers [4,5,8,14,15]. It includes an SO_2 sublimation rate based on the surface temperature, internal energy (rotation and quantized vibration) modes, and a collision limiter scheme to increase the computational efficiency in the near continuum regime. Rotational radiative cooling of the SO_2 is modeled by summing the emission line intensities computed from the tabulated HITRAN absorption line intensities and has a timescale of ~250 s at 300 K. Vibrational radiative cooling is modeled by spontaneous emission from the vibrational bands. Since the mean lifetime for decay from the ν_3 (1362 cm^{-1}) SO_2 vibrational state is much smaller than the desired gas timestep, a substep method is utilized. The sublimation rate of SO_2 off the surface frost is computed using the vapor pressure at equilibrium and assuming unit sticking to the frost surface. Other particles have a constant sticking probability on the surface ranging from unity for a perfectly condensable gas to zero for a perfectly non-condensable gas. If a molecule does not stick, it is assumed to scatter diffusely off the surface.

Our previous plasma heating model [14] was crude; it only transferred translational and rotational energy equally to all the target molecules in a cell based on the local density and an energy transfer cross section. The plasma did not transfer momentum, dissociate, or directly excite the vibrational modes of the target molecules. However, Saur [16] argued that the atmospheric scale height should decrease (compress) on the upstream side (relative to the plasma flow) due to momentum transfer by the plasma flow past Io. Furthermore, while Io's atmosphere is a mix of SO_2, SO, O_2, O, and S, the original source of Io's atmosphere is SO_2 (and S_2 from plumes, not modeled here) that is then dissociated via plasma and photo-chemistry. It is this final atmospheric composition that we seek to obtain.

Figure 1a shows a schematic of the new 1-D atmospheric simulation and the major physical mechanisms now included. In the new plasma interaction model each additional improvement to the model is de-activated in sequence to quantify the relative effects of each physical mechanism on Io's vertical atmospheric structure. In the full model, ions (O^+ and S^+) and electrons from the torus enter the top of the domain. The ions undergo non-reactive collisions and resonant charge exchange; the electrons undergo elastic, ionization, and dissociation collisions with the neutrals in order to model Joule heating of the atmosphere. In addition, the charged particles drift at ~57 km/s towards the surface due to the jovian magnetic and electric fields. After resonant charge exchange in the exosphere [3], the fast neutral O and S atoms collide with other neutrals in Io's atmosphere independent of the local fields, sometimes undergoing dissociative collisions based on cross sections computed via MD/QCT [1, 11]. Finally, the atmosphere is assumed to be optically thin and the atmospheric molecules are allowed to photo-dissociate using the "quiet" sun photo-dissociation rates and product thermal energies [17]. Figure 1b shows a subset of the included cross sections as used in the code as a function of the relative velocity. In general, curve-fits and linear interpolation are used between the experimental and MD/QCT data points.

To correctly model the fast particles, a thermal gas timestep, $\Delta t_{gas,}$ and a much smaller fast particle timestep, Δt_{fp}, were utilized. First the slow, thermal gas particles are moved and collided and then, holding the thermal gas particles fixed in space, the fast particles are moved and collided $\Delta t_{gas}/\Delta t_{fp}$ times. At the start of each gas timestep all ions,

electrons, and any neutral particles that are travelling at speeds greater than 2 km/s are treated with the fast particle timestep, the rest are treated using the gas timestep.

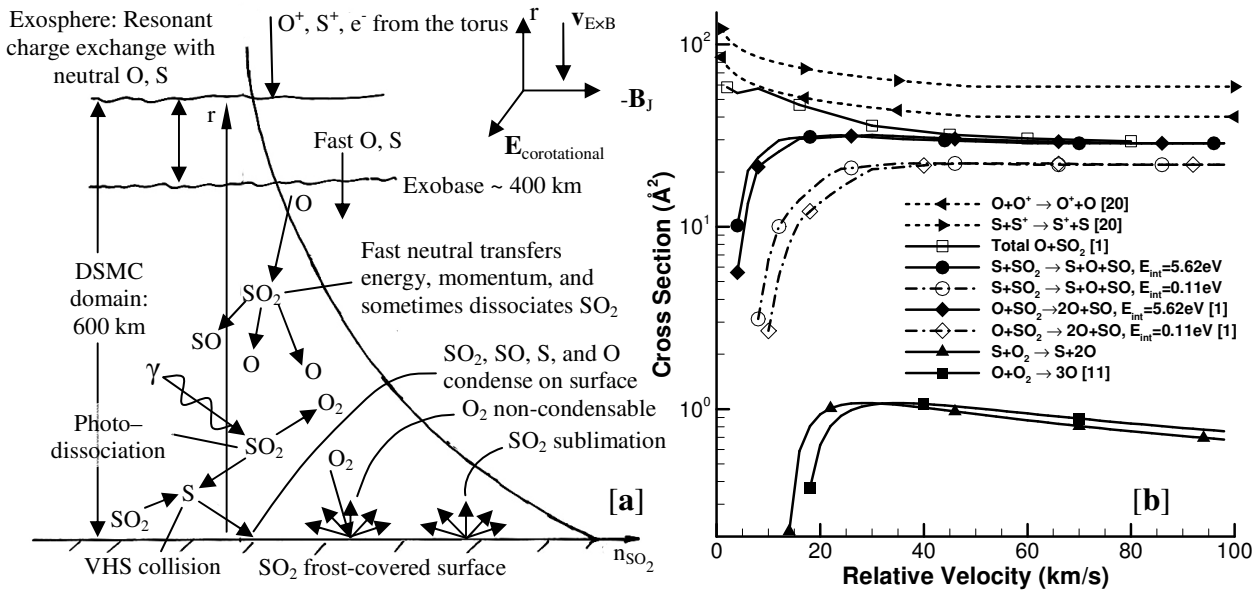

FIGURE 1: (a) Schematic of the major physical processes modeled in the atmospheric simulations (electron interactions are included but not shown, see [10]). Ions from the torus stream radially downward towards the subliming surface and undergo charge exchange above the exobase creating fast neutral O and S atoms which then compress the atmosphere and dissociate the SO_2. (b) Cross section versus relative collision energy for several of the included reactions taken from indicated references.

Since Io's orbital period is slower than Jupiter's rotational period, the jovian magnetic field (and therefore plasma torus) sweeps past Io at 57 km/s and in Io's reference frame a corotational electric field is established such that, upstream, the charged particles drift at 57 km/s relative to Io. The bulk plasma density upstream of Io is ~3600 cm^{-3} and has an ion temperature of 100 eV and an electron temperature of 5 eV [18]. In the current 1D model, we apply constant external magnetic (1800 nT) and electric (0.0124 V m^{-1}) fields which then cause the charged particles to **E×B** drift at 57 km/s down into our domain at the sub-plasma point of Io. Modeling the charged particles in addition to fast neutrals created via charge exchange is important because of the additional Joule heating and the electron chemistry. In particular, electron ionization of O and S atoms (which are then swept away) should dramatically change those species' densities at high altitudes. The current model including ions and electrons is an upper limit for the effect of Joule heating and chemistry since the fields are held constant. In reality the fields will adjust due to Io's mass loading of the torus such that, at lower altitudes, the drift towards the surface is slower and much (~80%) of the plasma flow will be diverted around Io and the (lower) atmosphere [19].

In the 1D model, ambipolar diffusion is neglected since it results in a field perpendicular to the magnetic field and therefore will cause a drift perpendicular to the radial direction. Since this diversion of the flow should reduce the plasma flux to lower altitudes, the current 1D simulations with charged particles offer an upper bound on the plasma's effect on Io's atmosphere and the simulations that only include fast neutrals offer a lower bound on the plasma effect. Future simulations in our 3D code [8] will incorporate the ambipolar field. In the current model we assume each electron's motion is linked to a corresponding ion [20] whose motion is effected by the Lorentz force and Io's gravity. This linkage exactly enforces charge neutrality and the electrons retain their own velocity components which are then used during collisions with the neutral gas. For collisions between dissimilar ions and neutrals the elastic collision cross section can be approximated using the VHS model at the typical collision energies (> 1 eV) present at Io [9]. Resonant charge exchange for O^+ and S^+ is included via an analytic curve-fit [21]. For electrons, elastic cross sections were included for collisions with all the neutral species. In addition, the model included electron-impact cross sections for dissociation (SO_2) and for ionization (SO_2, O, and S) [10].

After resonant charge exchange, fast neutral O and S atoms stream through the atmosphere, occasionally colliding with the slower, nearly thermal gas. These energetic collisions have sufficient energy to dissociate molecules and yet no experimental data on reaction rates at these energies exists. Therefore, the O+SO_2 reaction cross section has been modeled by MD/QCT simulations at eight relative velocities and five internal energies of the target SO_2 [1]. Similar MD/QCT collision data for high velocity O+HCl collisions were used in DSMC simulations

of a lateral side jet on a rocket [22]. In the current work, the DSMC simulation includes the $O+SO_2 \rightarrow 2O+SO$ reaction cross section versus internal energy at a specific relative velocity through polynomial curve-fits to the MD/QCT dissociation cross section data at 4, 8, 16, 30, 45, 60, and 80 km/s. Note that the $O+SO_2 \rightarrow \{O+S+O_2$ and $3O+S\}$ reaction paths are currently not included; the MD/QCT simulations found that below ~16 km/s these pathways are negligible and at 80 km/s they only comprise 10% of all dissociation reactions. Below 4 km/s there is insufficient energy to dissociate the SO_2 except at very high internal energies, therefore we assume that no dissociation occurs. For cross sections at relative velocities between the MD/QCT data points, linear interpolation is used and above 80 km/s we assume that the dissociation cross section is constant.

In addition to the reaction cross section, MD/QCT can be used to compute the $O+SO_2$ total collision cross section. This is desired since the VHS parameters used for low velocity collisions are from fits to low temperature viscosity data and thus the total cross section is under-predicted at high velocities (>2 km/s) by the VHS model. The result is that above a certain relative velocity and initial internal energy threshold for the SO_2 molecule, the MD/QCT reaction cross section exceeds the VHS cross section. Future work will compute viscosity based VHS parameters [21] for the $O+SO_2$ collision pair which better fit the MD/QCT collision data in the high velocity regime. In the current work, we approximate the total cross section in the following way. Above 2 km/s the total collision cross section is set equal to the MD/QCT reaction cross section plus the viscosity based cross section that includes all non-reactive collisions [1]. Since the total collision cross section is mostly independent of the initial SO_2 internal energy, we set it equal to the sum of the reaction and viscosity cross section for an initial SO_2 internal energy equal to 99% of the dissociation energy so that the total collision cross section is a function of relative velocity only. Given a collision event, a dissociation reaction occurs if a random number is less than the ratio of the dissociation cross section to the total collision cross section.

Since O_2 is non-condensable at Io's surface temperatures, destruction of O_2 via high velocity $O+O_2$ collisions is important. These collisions were previously modeled using a classical MD simulation and curve fit parameters to the simulation results for dissociation provided in [11]. Once again it was necessary to sum the diffusion cross section and the dissociation cross section in order to obtain a total collision cross section for use in our DSMC code.

The plasma torus is mainly composed of 2/3 O^+ and 1/3 S^+ and so accounting for the $S+SO_2$ collisions is important. Currently, MD/QCT simulations have not been run for these collisions; however, at these relative velocities the dissociation cross section should be mostly independent of the collider's potential surface. Therefore, we scale the $S+SO_2$ dissociation cross section so that the $S+SO_2$ cross section is equal to the $O+SO_2$ cross section for the same total collision energy (internal plus kinetic energy).

In all cases the domain extended to an altitude of 600 km above which a 1000 km "buffer" cell was placed. Each timestep, particles in the "buffer" cell are moved (but not collided) and, if a particle reaches the top of the "buffer" cell, then the particle is deleted. An adaptive grid was used that distributed the domain's 500 cells among 10 radial segments spaced such that each contained ~10% of the atmospheric mass. In each segment, the grid spacing was linearly stretched such that the ratio of the cell size to the mean free path was equal to a constant (< 2) at the bottom and top of each segment. A steady state value of $\sim 10^6$ simulation particles was used so that even the minor neutral species had more than several molecules per cell where the gas is collisional.

RESULTS

Several cases were simulated in order to examine the relative importance and effect of the various physical processes: Case 1 is the original plasma heating model, Case 2 simulates the nominal fast neutral flux, Case 3 simulates a lower flux of fast neutrals, Case 4 adds photo-dissociation to Case 2, Case 5 simulates the nominal charged particle flux including **E×B** drift and charge exchange with photo-dissociation, and Case 6 simulates a lower charged particle flux than Case 5. In these simulations nominal flux refers to an upstream density of 3600 cm^{-3} and a bulk velocity of 57 km/s whereas the lower flux refers to 20% of the nominal flux since prior modeling found that ~20% of the co-rotating plasma reaches Io's exobase [19]. All cases were run at a surface temperature of 115K.

Figure 2a shows the total number density versus altitude. It is seen that allowing the ions and electrons to re-accelerate to a constant **E×B** drift dramatically effects the vertical density profile of the atmosphere. Cases 5 and 6 with ions and electrons heating the atmosphere have much lower densities near the surface and much higher densities at high altitudes, consistent with increased heating of the gas. While the current charged particle model overestimates joule heating, the large differences between density profiles with and without charged particles indicates that it is probably important and it will be treated more accurately in our future 2D and 3D simulations. For the simulations with just neutrals, the various physics serve to alter the atmospheric structure in two distinct regions around ~3 km and above 100 km in altitude; however, it is notable that the previous plasma model that only

included heating compares surprisingly well with all the density profiles using a much more complex plasma model. The first region at 3 km altitude results from the competition between radiative cooling and plasma heating of the atmosphere. Below 3 km there is negligible plasma energy deposited into the gas and the atmosphere radiatively cools fast enough such that the density must increase with altitude in order to maintain hydrostatic exponential falloff in the pressure. Examining the inset for Cases 2 and 3 (nominal and lower flux), one can see the effect of the plasma pressure on the gas. In Case 2 the larger flux of fast neutrals compresses the upper atmosphere more than in Case 3 resulting in a 30% increase in total density at 2 km and a steeper fall-off in density immediately above ~3 km where the density for the lower flux now exceeds that of the nominal flux. The density in Case 4, which includes photo-dissociation, is more inflated than Case 2, as one would expect due to the excess energy deposited via photo-reactions. The second region above ~100 km is related to whether the atmospheric density has dropped far enough such that it is collisionless on the timescale of ballistic motion (~100 s). Again, photo-dissociation is seen to inflate the atmosphere, though this is because there are more light species with larger scale heights with photo-dissociation.

Figure 2b shows the number density of the neutral gas versus altitude for Case 4. The overall densities are similar to those shown in [6] accounting for the different surface temperatures, photo-dissociation rates, and that previously SO was assumed non-condensable. The main difference seems to be that their drop-off in O and S density near the surface extends to ~40 km, whereas in our simulations the drop-off extends to ~4 km. Presumably this difference is because in our 1D model there is virtually no vertical velocity (< 0.1 m s^{-1}) below ~50 km; however, in the 2D simulation presented in [6], substantial vertical and tangential velocities develop that convect the dayside atmosphere to the low-pressure nightside. This vertical velocity would drastically reduce the diffusion towards the surface of O and S produced in the upper atmosphere. In the upper atmosphere the scale heights slightly separate, with the lower mass particles having larger scale heights as one would expect for a hydrostatic atmosphere. However, the scale heights are not completely decoupled from the heavy SO_2 because the lighter species are produced through SO_2 chemistry. Specifically, if the gases were completely decoupled, the ratio of O to SO_2 scale height would be equal to the inverse of their mass ratio (and independent of the gas temperature), or 4 for O and SO_2; however, the upper atmosphere scale height for O is ~280 km and for SO_2 is ~240 km giving a ratio of ~1.17.

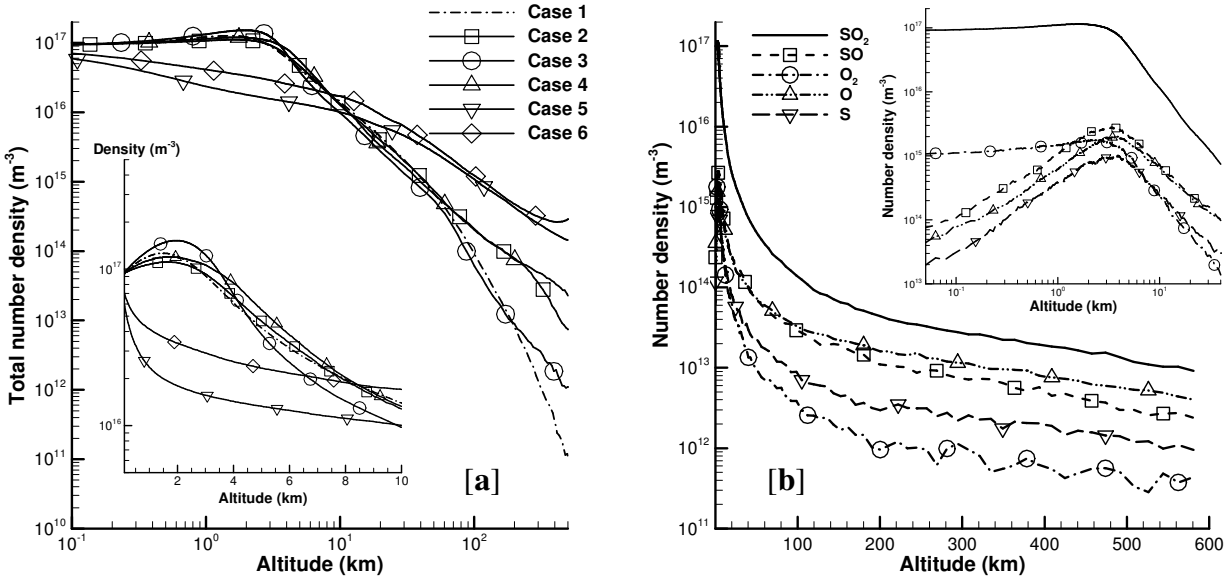

FIGURE 2: (a) Total number density and mean time between collisions versus altitude. The total number density is seen to change relatively little for the various cases. (b) The number density of the neutral gas species versus altitude for Case 4. We see that the density for non-condensable O_2 does not drop off near the surface unlike for the other condensable daughter species (SO, O, and S). Once the atmosphere is collisionless the species' scale heights are seen to slightly separate.

Figure 3a compares the vertical structure of the translational temperature for the various cases. It is seen that allowing the ions and electrons to reaccelerate to a constant **E×B** drift allows the plasma to deposit significant energy all the way to the surface. Note, that Case 5 and 6 have much lower gas densities near the surface (Fig. 2a) because the gas is not in thermal equilibrium with the surface; the higher gas temperature near the surface increases the flux of gas to the surface while the sublimation rate is fixed by the surface temperature. While a lower flux corresponds to a lower temperature, continual reacceleration to a constant drift speed means that the energy in the plasma does not decay significantly towards the surface. The old plasma model (Case 1) matches the translational

temperature remarkably well, especially in the lower atmosphere, lying between temperatures for the two plasma fluxes. It is seen that, below ~100 km where the atmosphere is collisional, the low plasma flux case is generally colder than the nominal flux case. Interestingly, above ~200 km the temperature with photo-dissociation is less than the temperature with just fast neutrals. Most likely this is because photo-dissociation creates more light particles whose larger scale heights result in more mass at higher altitudes and whose cross sections with the incoming plasma are smaller (and less refined in our model since, in general, they are minor species). Also, for the hotter cases we observe evaporative cooling as the hottest gas has sufficient energy to escape Io. In figure 3b it is seen that, because the original plasma model did not deposit energy into the vibrational modes, it does not model the vibrational temperature correctly once the atmosphere is sufficiently collisionless. At high altitudes in Fig. 3c, it can be inferred that the internal energy of the molecules is not insignificant and therefore accounting for the internal energy when modeling the dissociation rate is important.

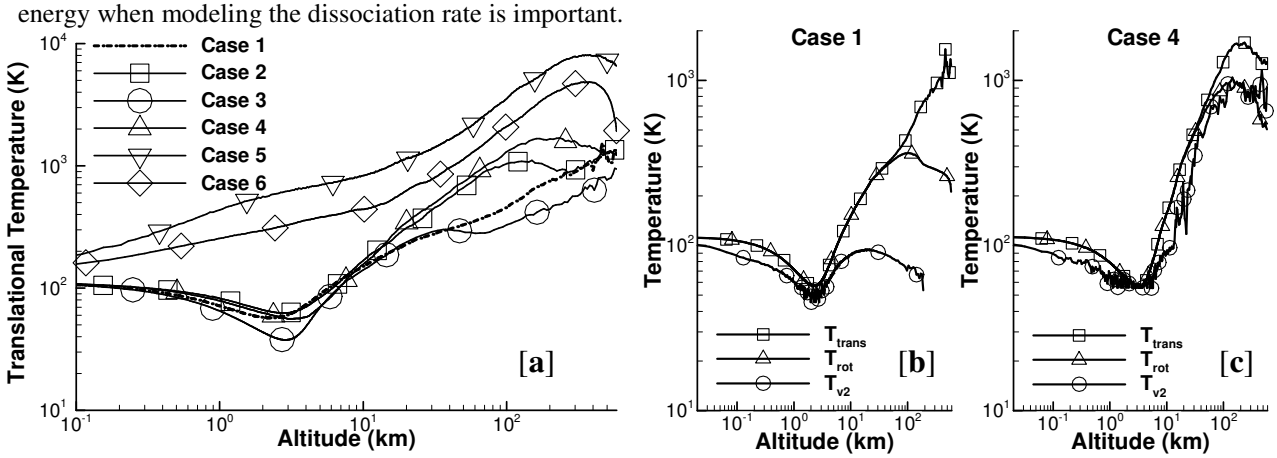

FIGURE 3: (a) Translational temperature of the neutral gas mixture versus altitude for the various cases. Once the gas density drops enough that it is collisionless on the timescale of ballistic motion, the gas no longer remains in thermal equilibrium and the plasma collisions. (b) Comparison of the translational, rotational, and ν_2 (518 cm^{-1}) vibrational temperatures for Case 1 and Case 4. The original plasma heating model does not correctly model the vibrational temperature of the gas at high altitudes.

ACKNOWLEDGMENTS

This work supported by NASA grants through the Planetary Atmospheres and Outer Planets Research programs.

REFERENCES

1. H. Deng, C.H. Moore, D.A. Levin, and D.B. Goldstein, *27th Rarified Gas Dynamics Symposium* (2010).
2. A.P. Ingersoll, *Icarus* **81**, 298–313 (1989).
3. M.K. Pospieszalska and R.E. Johnson, *JGR* **101 E3**, 7565–7573 (1996).
4. C.H. Moore, D.B. Goldstein, P.L. Varghese, L.M. Trafton, and B.D. Larignon, *Icarus* **201**, 585–597 (2009).
5. J.V. Austin and D.B. Goldstein, *Icarus* **148**, 370–383 (2000).
6. W.H. Smyth and M.C. Wong, *Icarus* **171**, 171–182 (2004).
7. K.L. Jessup, J.R. Spencer, G.E. Ballester, R.R. Howell, F. Roesler, M. Vigel, and R. Yelle, *Icarus* **169**, 197–215 (2004).
8. A. Walker, S. Gratiy, D. Goldstein, C. Moore, P. Varghese, L. Trafton, D. Levin, B. Stewart, *Icarus* **207**, 409–432 (2010).
9. G.G. Chernyi, S.A. Losev, S.O. Macheret, and B.V. Potapkin, Progress in Astronautics and Aeronautics, **196** (2002).
10. C. Moore, K. Miki, D. Goldstein, K.Stapelfeldt, P. Varghese, L. Trafton, and R. Evans, *Icarus* **207**, 810–833 (2010).
11. R.E. Johnson, M. Liu, and C. Tully, *Planetary and Space Sci.* **50**, 123–128 (2002).
12. R.E. Johnson, *Space Sci. Rev.* **69**, 215–253 (1994).
13. G.A. Bird, *Molecular Gas Dynamics and the Direct Simulation of Gas Flows*, Oxford: Oxford Univ. Press., 1994.
14. J. Zhang, D.B. Goldstein, P.L. Varghese, L. Trafton, C. Moore, and K. Miki, *Icarus* **172**, 479–502 (2004).
15. B.D. Stewart, D.B. Goldstein, P.L. Varghese, L.M. Trafton, and C.H. Moore, *47th* AIAA, #2009–266.
16. J. Saur, F.M. Neubauer, D.F. Strobel, and M.E. Summers, *JGR* **107**(A12), 1422, doi:10.1029/2001JA005067
17. W.F. Huebner, J.J. Keady, and S.P. Lyon, *Astrophysics and Space Sci.* **195**, 1–294.
18. F. Bagenal, T. Dowling, and W. McKinnon, *Jupiter: The Planet, Satellites and Magnetosphere.* 513–536 (2004).
19. J.A. Linker, M.G. Kivelson, and R.J. Walker, *Geophys. Res. Lett.*, **16**, 763–76 (1989).
20. G.A. Bird, *AIAA/ASME 4th Thermophysics and Heat Transfer Conference*, AIAA Paper #86–1310 (1986).
21. B.M. Smirnov, *Physica Scripta*, **61**, 595–602 (2000).
22. T. Ozawa, D.A. Levin, and I.J. Wysong, *Phys. of Fluids* **19**, 056102 (2007).